

# THE 4TH INTERNATIONAL CONFERENCE ON ALUMINUM ALLOYS

## EFFECT OF TEXTURE AND PRECIPITATES ON MECHANICAL PROPERTY ANISOTROPY OF Al-Cu-Mg-X ALLOYS

B. Skrotzki, E.A. Starke, Jr., and G.J. Shiflet  
Department of Materials Science and Engineering, University of Virginia, Thornton Hall,  
Charlottesville, VA 22903-2442, USA

### Abstract

The effect of texture on precipitation of  $\Omega$  and  $\theta'$  in Al-Cu-Mg-X sheet material and the associated influence of anisotropy on mechanical properties have been investigated. In addition, the effect of an applied stress on nucleation and growth of the precipitates has been examined. The Taylor factor has been calculated to separate the crystallographic texture effect from that due to precipitates.

### Introduction

Prerequisite for plastic yielding in a polycrystalline material is that the critical resolved shear stress is reached on a number of slip systems in order to maintain compatibility across the grain boundaries. It is supposed that every grain undergoes the same deformation as the aggregate. This requires an external stress which depends on its direction and the crystallographic texture of the material. Most treatments of this problem are based on the theory of Taylor [1] and Bishop and Hill [2] and relate to single crystals. Taylor derived a factor,  $M$ , which relates the stress necessary for plastic flow to the critical resolved shear stress of the crystal. It predicts whether the slip is easy or difficult and is a function of the crystal orientation and the texture of the material. The Taylor-factor

$$M = \frac{\delta\gamma_T}{\delta\varepsilon} \quad (1)$$

is the smallest total shear strain necessary to give total macroscopic strain. For a random crystal orientation  $M$  is equal to 3.06 using the Taylor method. The effect of texture strengthening can be considerable. Compared to randomly oriented crystals it can be increased by 20% or decreased by 25% if a strong  $\{111\}$  or  $\{100\}$  fibre texture is present [3]. For processing sheet material this means that the properties can be considerably anisotropic.

If the single phase material is strengthened by second phase particles the plastic anisotropy is usually changed. The effect depends on shape and habit planes of the precipitates and may reduce or increase anisotropy [4-8]. In addition, deformation prior to aging affects nucleation of precipitates that have large coherency strains or interfacial energies. If the dislocation structure which results from deformation is not uniform, nucleation of precipitates won't occur with the same frequency on all possible habit planes. Also, for applications where both stress and moderate temperature increases occur, shifts in phase fields and coarsening behavior of precipitates may be affected [9-12].

## Experimental Procedure

The compositions of the investigated alloys are given in Table I. The alloys were cast at the Alcoa Technical Center as 6" x 16" x > 60" ingots, preheated and rolled to 0.125" thick sheet.

Table I. Chemical composition [wt.%] of the investigated sheet material

Alloy	Cu	Mg	Mn	Ag	Zr	V	Fe	Si	Al
A	5.83	0.52	0.30	---	0.14	0.10	0.05	0.05	balance
B	5.75	0.52	0.30	0.49	0.16	0.09	0.06	0.05	balance

Texture measurements have been carried out at half sheet thickness after solution heat treatment at 520°C for 1 h of the as received material. From {111}, {200} and {220} pole figures the Orientation Distribution Function (ODF) has been calculated and used to determine the fully constrained Taylor factor as a function of orientation.

The solution heat treated material has been aged with and without prestraining at  $T = 163^\circ\text{C}$ . The precipitate structure has been characterized by TEM, using a Philips EM 400 T microscope. Tensile tests have been carried out in RD, 45° to RD and TD for the solution heat treated, peak aged (T6) and prestrained and peak aged (T8) condition. The amount of prestraining was 8% for the silver free alloy (A) and 2% for the silver containing alloy (B).

Creep tests have been made for the silver containing alloy (B) to determine the effect of an applied stress on nucleation and growth of the precipitates. A constant load (40% of room temperature yield strength) was applied at a constant temperature of  $T = 160^\circ\text{C}$  to solution heated and peak aged specimens, respectively. As the deformation is very low the stress  $\sigma$  is considered as constant. The microstructure was characterized by TEM after 10 and 100 h creep. The approach of Underwood [13] for projected images has been applied to determine the volume fraction and number density of precipitates. It was assumed that the precipitates are disk shaped. Convergent beam electron diffraction was employed to determine specimen thickness.

## Results and Discussion

### Texture

Texture measurements of the solutionized and completely recrystallized alloys (mean grain size was 54  $\mu\text{m}$  for alloy A and 38  $\mu\text{m}$  for alloy B) showed a completely random crystal distribution. This is not the normal recrystallization texture of aluminum alloys. The reason for this may be associated with the high volume fraction of constituent phases (size  $\approx 9 \mu\text{m}$ ) which could have resulted in deformation zones during rolling. These deformation zones can serve as recrystallization sites during subsequent heat treatment and result in a random texture [14].

### Microstructure and Mechanical Properties

In alloy A the strengthening phases are  $\Theta''$  and  $\Theta'$  ( $\text{Al}_2\text{Cu}$ ), respectively, which precipitate on  $\{100\}_{\text{Al}}$  planes. The strengthening phases in alloy B are  $\Theta''$  and  $\Theta'$ , as in A, but also includes  $\Omega$  with a composition close to  $\text{Al}_2\text{Cu}$ . The habit plane of  $\Omega$  is  $\{111\}_{\text{Al}}$ . Both types of precipitates are plate shaped (Fig. 1). Prestraining of 2% does not change the precipitate microstructure except that the dislocation density is increased. Fig. 2 shows the age hardening response after aging at  $163^\circ\text{C}$ . The maximum hardness for the silver free alloy occurs at about 10 h. After longer aging times the hardness decreases. This is different from the silver containing alloy, which reaches its maximum

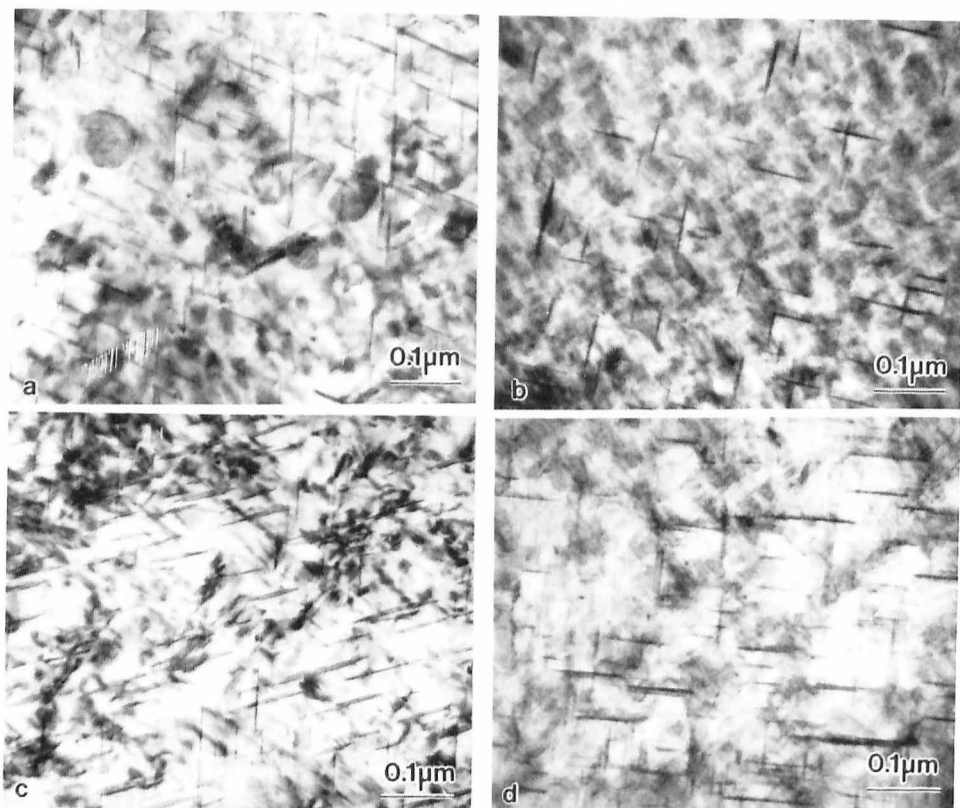


Figure 1. Microstructure of alloy B. (a)  $\Omega$  and (b)  $\Theta'$  precipitates after 20 h/163°C aging; (c)  $\Omega$  and (d)  $\Theta'$  precipitates after 2 % prestraining and 16 h/163°C. ( $[110]_{Al}$  zone axis for  $\Omega$  and  $[100]_{Al}$  zone axis for  $\Theta'$  precipitates)

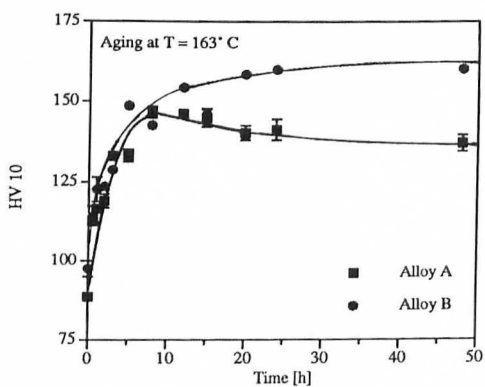


Figure 2. Age hardening response after aging at  $T = 163^\circ\text{C}$ .

hardness at about 20 h but the hardness remains constant after further aging due to the higher thermal stability of the  $\Omega$  phase.

Both alloys showed fairly isotropic behavior in uniaxial tensile tests. The silver free alloy has a low strength in the solution heat treated condition. The peak aged condition shows a considerable increase of the tensile yield strength which can be further raised by 8% prestraining (Fig. 3a). This shows that the strength of the silver containing alloy can be nearly reached by alloy A, but that the thermal stability is lower. Peak aging the silver containing alloy (B) provides a considerable increase of the yield strength compared to the solution heat treated condition (Fig. 3a). This is due to the combined precipitation of  $\Theta'$  and  $\Omega$ . Prestraining of 2% does not lead to a further increase. The ultimate tensile strength reached values between 500 and 540 MPa for the aged conditions and about 400 MPa for the solution heat treated condition.

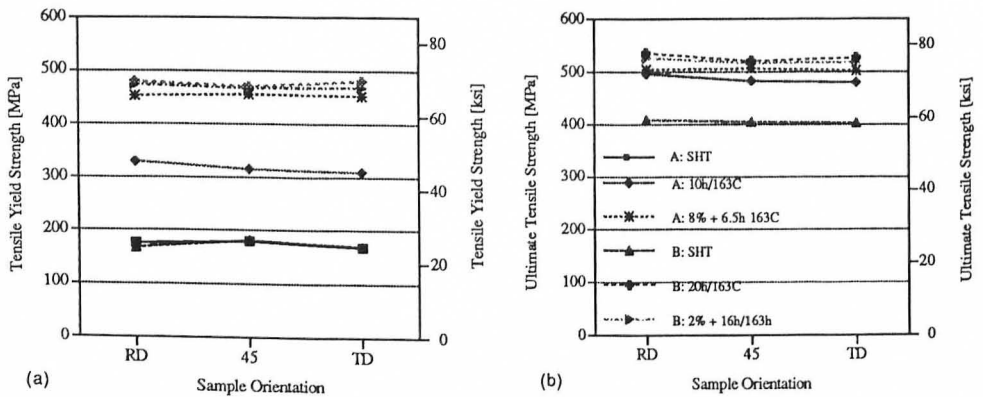


Figure 3. Mechanical properties from tensile tests for different sample orientations. (a) tensile yield strength (b) ultimate tensile strength

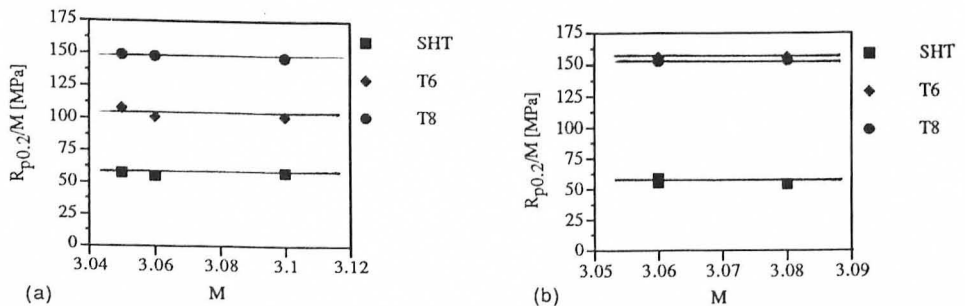


Figure 4. Normalized yield strength,  $R_{p0.2}/M$ , vs. Taylor Factor, M. (a) alloy A (b) alloy B.

The sheet material is isotropic in all conditions. This was expected for the solution heat treated condition because the texture measurements showed random crystal orientation. It was somewhat surprising for the (prestrained and) aged conditions since plate precipitates on a particular habit plane of the matrix normally affects the anisotropy. It has been found that precipitates on {111} planes normally increase and those on {100} planes normally decrease anisotropy [4,5]. Since both types of precipitates are present in the silver containing alloy, it is assumed that their effects approximately cancel each other.

The Taylor Factor,  $M$ , has been calculated from the ODF. As the texture is random, it is not surprising that  $M$  is close to 3.06. Fig. 4 shows the normalized yield strength,  $R_{p0.2}/M$ , vs. Taylor Factor,  $M$ . The results indicate that the normalized yield strength is independent of  $M$ . The increase of  $R_{p0.2}/M$  is due to the precipitation hardening effect. As fully recrystallized specimens were used for aging treatment, the texture should remain unaffected.

### Nucleation and Growth under Stress

The effect of an applied stress on nucleation and growth of precipitates has been investigated separately for alloy B. An external stress has been applied to both solutionized and peak aged specimens. For a quantitative characterization of the resulting microstructure, the volume fraction of precipitates, the number of particles per volume, the particle diameter and thickness have all been experimentally determined. Figs. 5a - d show the results.

Prestraining (T8) increases the volume fraction of both types of particles but there is no change in the number density, compared to the peak aged condition (T6). This means that growth kinetics were accelerated. As  $\Theta'$  precipitates prefer to nucleate at dislocations, it was expected that its number density might increase, but this was not observed.

Particle growth under stress (T6 + creep) results in a higher volume fraction of  $\Omega$  after a given heat treatment time, particularly after long aging times (for 10 h aging the error bar is too large to get a clear result). This is due to the increasing number density compared to T6. Apparently, there is further nucleation of particles. The volume fraction of  $\Theta'$  increases, too, but this is due to the increased size of the particles. The number density remains nearly unchanged. Assuming that the phase boundaries are not changed due to the applied stress, accelerated nucleation and growth rates are responsible for the increase in volume fraction after a specific time.

Nucleation and growth under stress (SHT + 10 h, 100 h creep) leads to a high number density of  $\Omega$  particles. After 10 h aging the particles are still in the underaged condition. 100 h aging leads to a lower number density of  $\Omega$  and  $\Theta'$ . For  $\Omega$  the stage of Ostwald ripening has been reached (constant volume fraction of  $\Omega$ , decreasing number density). The volume fraction of  $\Omega$  is not much affected compared to the T6 condition. The volume fraction of  $\Theta'$  is somewhat lower after 10 h aging compared to T6 (underaged condition). After 100 h aging it increases considerably but the error bar is very large.

The size of the  $\Omega$  particles is nearly unchanged for all conditions, except for solutionized and 10 h aged condition, which is underaged.  $\Theta'$  behaves differently. It is obvious that the particles ripen during longer aging treatments. This means that the  $\Omega$  phase, which is the equilibrium phase, is very stable compared to  $\Theta'$ . At these times and temperatures  $\Theta'$  may be dissolving at the expense of equilibrium  $\Theta$ .

The large scatter of the volume fraction measurements of  $\Theta'$ , especially for the crept samples, was rather unsatisfactory. Therefore, further analysis was done. The volume fraction was determined separately for every habit plane and the angle between the precipitates and the direction of the applied load has been measured for solutionized samples. The results are illustrated in Fig. 6. Fig. 6a shows that the higher volume fraction of  $\Theta'$  precipitates occurs at lower angles to the applied

stress (<math>40^\circ</math>), particularly after 100 h aging. This means that there is preferred nucleation and growth of one habit plane. On the other hand, this was not observed for  $\Omega$  precipitates (Fig. 6b).

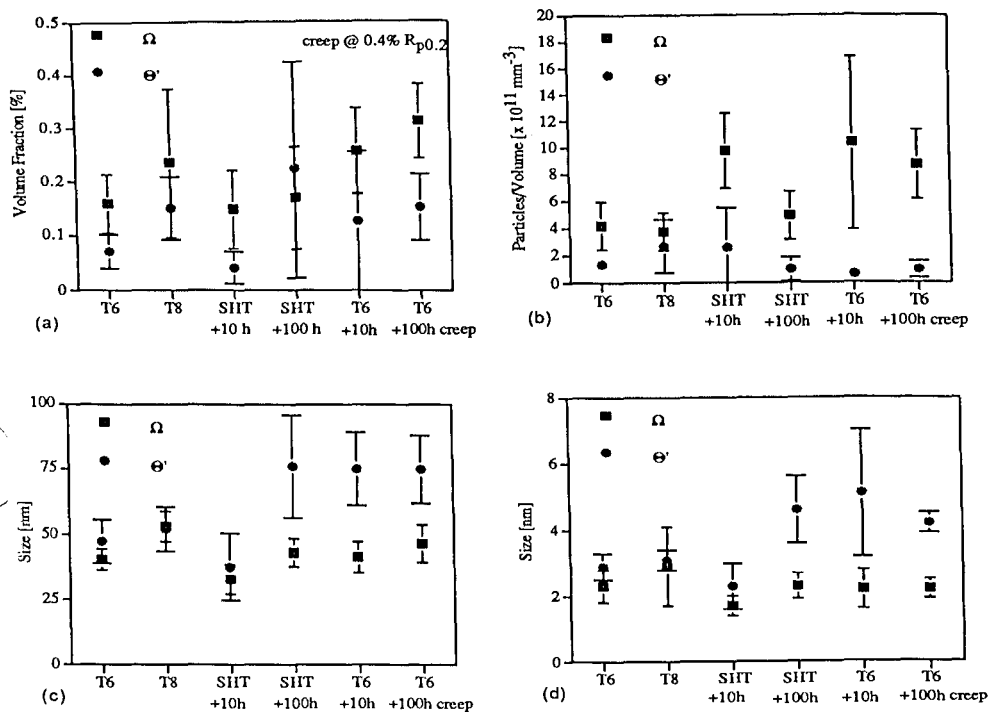


Figure 5. Quantitative characterization of the microstructure of alloy B. (a) Volume fraction (b) number density (c) diameter and (d) thickness of  $\Omega$  and  $\Theta'$  precipitates in T6 and T8 treatment. Aging under stress was done in a creep machine at 160°C. Applied stress was 40% of room temperature yield strength.

The applied tensile stress may provide elastic changes on the lattice dimensions of the matrix. As a result, the coherency strains between matrix and precipitates decrease or increase depending on the resolved stress. If this is true, the question arises, why  $\Omega$  is not affected. Previous investigations of  $\Theta'$  and  $\Omega$  precipitations have shown that  $\Theta'$  shows a relatively low positive strain field for more than 3.5 unit cell thickness (2  $\Theta'$ -cells: -4.3%, 3.5  $\Theta'$ -cells: +0.5%, 5.5  $\Theta'$ -cells: +1.3%, 7  $\Theta'$ -cells: +0.5%, ...) [15], whereas  $\Omega$  shows a large (~9%) negative strain field [16]. Depending on the orientation of the precipitate plate with respect to the projected component of force, an applied tensile stress leads to a relaxation of the strain field around  $\Theta'$  but to an increased strain field around  $\Omega$  (Fig. 7). Therefore the growth of  $\Theta'$  particles becomes easier once a certain thickness is reached (> 3.5 unit cells). This means that after nucleation of  $\Theta'$  the growth of certain orientations is favored because the particle fit in the matrix is improved.

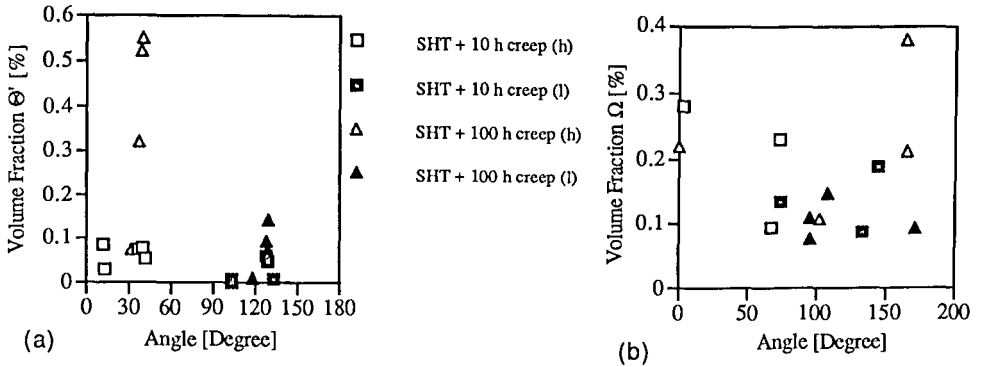


Figure 6. Volume fraction of precipitates in respect to angle between habit plane and direction of applied stress for alloy B. (a)  $\Theta'$  (b)  $\Omega$  phase. Open symbols for higher (h), full symbols for lower (l) volume fractions. Samples were aged under stress after solution heat treatment.

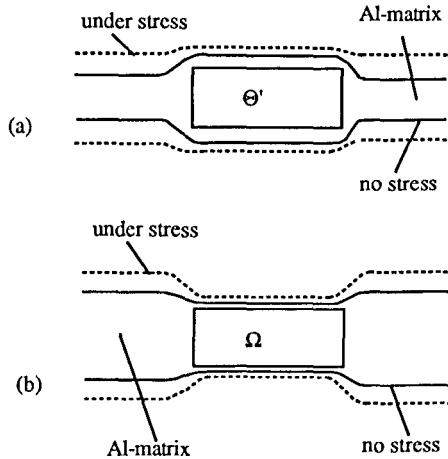


Figure 7. Relaxation of the strain field around  $\Theta'$  precipitate (a) and increasing strain field around  $\Omega$  precipitates (b) due to externally applied stress.

A second possibility is the effect of stress on the diffusion necessary for growth. Growth is largely volume diffusion controlled. The rates of diffusion depend on the stress field as well as upon compositional gradients. It is assumed that in the present case diffusion has only a secondary effect which would manifest itself in precipitate morphology (e.g., aspect ratio). By changing the strain field around the ledges the diffusion path and the equilibrium shape might be changed but this does not fully explain the favored growth on certain habit planes.

Hosford and Agrawal [17] found that in a binary Al-4% Cu single crystal under tensile stress parallel to [100]  $\Theta'$  is precipitated preferentially on the cube plane perpendicular to the direction of tensile stress and inhibited on the two other cube planes, i.e. the higher volume fraction is observed at higher angles. This is different from the results obtained in this work. In the present

case a ternary alloy was investigated in which two different types of precipitates were observed. The elastic interaction between the closely spaced precipitates,  $\Theta'$  and  $\Omega$ , with opposite misfit may make predictions difficult, especially since  $\Omega$  has large strain fields. Therefore, it may be expected that the strain field around  $\Theta'$  is different compared to binary alloys because the microstructure and elastically interacting strain fields are more complex. In addition, Hosford and Agrawal found that there is a threshold stress for noting an effect on precipitate morphology. This is interesting for the unchanged  $\Omega$  particles. It is possible that in the present case the applied stress is too low if there are different threshold stresses for different types of particles.

Comparable data for samples in T6 condition after aging under stress are not yet available but it is assumed that similar mechanisms occur.

#### Acknowledgement

The authors wish to thank NASA-Langley Research Center for providing funding under Grant No. NAG-1-745, Dennis Dicus, program monitor.

#### References

1. G.I. Taylor, J. Inst. Metals **62** (1938), 307.
2. J.F.W. Bishop and R. Hill, Phil. Mag. **42** (1951), 414.
3. G.Y. Chin and W.L. Mammel, Trans. Metall. Soc. AIME **245** (1969), 1211.
4. W.F. Hosford and R.H. Zeisloft, Metall. Trans. **2** (1972), 113.
5. P. Bate, W.T. Roberts and D.V. Wilson, Acta Met. **29** (1981), 1797.
6. P. Bate, W.T. Roberts and D.V. Wilson, Acta Met. **30** (1982), 725.
7. L.M. Brown and W.M. Stobbs, Phil. Mag. **23** (1971), 1185.
8. L.M. Brown and W.M. Stobbs, Phil. Mag. **23** (1971), 1201.
9. W.C. Johnson and C.S. Chiang, J. Appl. Phys. **64** (1988), 1155.
10. C.S. Chiang and W.C. Johnson, J. Mat. Res. **4** (1989), 678.
11. W.C. Johnson, T.A. Abinandanan and P.W. Voorhees, Acta Met. Mat. **38** (1990), 1349.
12. T.A. Abinandanan and W.C. Johnson, Acta Met. Mat. **41** (1993), 17 & 27.
13. E.E. Underwood, Quantitative Stereology (Reading, MA: Addison-Wesley Publishing Company, 1970), 178.
14. J.C. Williams and E.A. Starke, Jr., "The Role of Thermomechanical Processing in Tailoring the Properties of Aluminum and Titanium Alloys", in: Deformation, Processing, and Structure, ed. G. Krauss (Metals Park, OH: ASM, 1984), 279.
15. U. Dahmen and K.H. Westmacott, Phys. Stat. Sol. (a) **80** (1983), 249.
16. R.W. Fonda, W.A. Cassada and G.J. Shiflet, Acta Metall. Mater. **40** (1992), 2539.
17. W.F. Hosford and S.P. Agrawal, Metall. Trans. **6A** (1975), 487.